p53 Determines Multidrug Sensitivity of Childhood Neuroblastoma

Chengyuan Xue,[1] Michelle Haber,[1] Claudia Flemming,[1] Glenn M. Marshall,[1] Richard B. Lock,[1] Karen L. MacKenzie,[1] Katerina V. Gurova,[2,3] Murray D. Norris,[1] and Andrei V. Gudkov[2,3]

[1]Children's Cancer Institute Australia for Medical Research, Randwick, New South Wales, Australia, and [2]Department of Cell Stress Biology, Roswell Park Cancer Institute and [3]Cleveland BioLabs, Inc., Buffalo, New York

Abstract

For pediatric cancers like neuroblastoma, the most common extracranial solid tumor of infancy, p53 mutations are rare at diagnosis, but may be acquired after chemotherapy, suggesting a potential role in drug resistance. Heavy metal–selected neuroblastoma cells were found to acquire an unusually broad multidrug resistance (MDR) phenotype but displayed no alterations in genes associated with "classic" MDR. These cells had acquired a mutant *p53* gene, linking p53 to drug sensitivity in neuroblastoma. We therefore generated p53-deficient variants in neuroblastoma cell lines with wild-type p53 by transduction of p53-suppressive constructs encoding either short hairpin RNA or a dominant-negative p53 mutant. Analysis of these cells indicated that (*a*) in contrast to previous reports, wild-type p53 was fully functional in all neuroblastoma lines tested; (*b*) inactivation of p53 in neuroblastoma cells resulted in establishment of a MDR phenotype; (*c*) p53-dependent senescence, the primary response of some neuroblastoma cells to DNA damage, is replaced after p53 inactivation by mitotic catastrophe and subsequent apoptosis; (*d*) knockdown of mutant p53 did not revert the MDR phenotype, suggesting it is determined by p53 inactivation rather than gain of mutant function. These results suggest the importance of p53 status as a prognostic marker of treatment response in neuroblastoma. p53 suppression may have opposite effects on drug sensitivity as determined by analysis of isogenic pairs of tumor cell lines of nonneuroblastoma origin, indicating the importance of tissue context for p53-mediated modulation of tumor cell sensitivity to treatment. [Cancer Res 2007;67(21):10351–60]

Introduction

The p53 tumor-suppressor pathway is the major cancer-preventive mechanism in mammals. Germ line mutations in p53 are associated with high cancer incidence in mice and men (1). p53 is mutated in ~50% of human malignancies and is functionally inactivated in the majority of cancers that retain wild-type *p53* gene due to overexpression of natural negative regulators of p53 of cellular (Hdm2 or Hdmx) or viral origin [E6 of human papillomavirus (HPV); refs. 2–4]. Restoration of p53 function results in toxicity in a majority of tumor cells, thus making it a prospective approach to cancer treatment. Loss of p53 provides tumor cells with a series of important selective advantages, including high tolerance to growth arrest– and death-inducing stimuli and genomic instability that promotes tumor progression by rapid acquisition of mutations (5).

In early studies, wild-type p53 was defined as a treatment sensitivity factor promoting apoptotic cell death of tumor cells under conditions of chemotherapy or radiotherapy (6). However, in later studies, it became clear that during progression tumors can acquire numerous mechanisms for suppressing apoptosis and that tumor response to treatment involves other mechanisms of death such as induction of senescence or mitotic catastrophe (7–9). In this latter case, p53-mediated growth arrest may lead to a rescuing effect under conditions of genotoxic stress, thereby preventing cells from prematurely entering a deadly mitosis. This dual role of p53 in treatment sensitivity has also been shown in normal tissues, where it may be either a strong proapoptotic factor or a survival factor in determining radiosensitivity of cells (10).

Drug resistance acquired in the course of therapy is the main obstacle to the successful treatment of many cancers, including childhood neuroblastoma, the most common extracranial solid tumor of childhood (11). A strong initial response is frequently followed by the appearance of multidrug resistant (MDR) variants. Although we have previously shown that the multidrug transporter MDR-associated protein 1 (MRP1) has an important role in this childhood malignancy (12, 13), another lesion acquired by drug-resistant neuroblastoma cells is mutant p53, suggesting the involvement of wild-type p53 in drug response (14). However, previous investigations in this area have been limited either to correlative studies or to modeling by using methods of p53 inhibition not reported in neuroblastomas (e.g., E6 of HPV). Moreover, this conclusion of p53 involvement in neuroblastoma conflicts with a number of studies showing a lack of activity of p53 in this disease due to its cytoplasmic sequestration (15–17).

We have addressed the role of p53 in determining drug response of neuroblastoma cells by studying an unusually broad MDR phenotype of neuroblastoma cells (IMR/KAT100) selected for resistance to potassium antimony tartrate (KAT). Our results show that *p53* acts as a drug sensitivity gene in some neuroblastoma cells by causing them to enter irreversible growth arrest (senescence), which is replaced by aberrant mitosis (mitotic catastrophe) and subsequent apoptosis in p53-deficient variants. This type of p53-dependent response to genotoxic stress is not universal to cancer cells and differs greatly among tumor cell lines of different tissue origin.

Materials and Methods

Cell lines and reagents. The following cell lines were used: human neuroblastoma [IMR-32, IMR/KAT100, SH-EP, SK-N-SH, SH-SY5Y, and SK-N-BE(2c)], renal carcinoma (RCC26b, RCC45, RCC54, and ACHN), osteosarcoma (U2OS), lung fibrosarcoma (HT1080), prostate cancer (LNCaP), breast carcinoma (MCF7), and colon carcinoma cell line HCT-116, as well as its p53-deficient variant HCT-116/p53−/−. All cells were cultured at 37°C in a humidified atmosphere of 5% CO_2 in air in either RPMI 1640 (RCC cells) or

Requests for reprints: Andrei V. Gudkov, Department of Cell Stress Biology, Roswell Park Cancer Institute, Elm and Carlton Streets, Buffalo, NY 14263. Phone: 716-845-3902; E-mail: andrei.gudkov@roswellpark.org or Murray D. Norris, Children's Cancer Institute Australia for Medical Research, P.O. Box 81, Randwick, 2031 Sydney, Australia. Phone: 61-2-9382-1823; E-mail: m.norris@unsw.edu.au.

doi:10.1158/0008-5472.CAN-06-4345

in DMEM. Cytotoxic drugs were purchased from manufacturers as follows: vincristine, etoposide (VP-16), and melphalan from Sigma; cisplatin, doxorubicin, and daunorubicin from Pharmacia & Upjohn; potassium antimony tartrate trihydrate from TJ Baker; teniposide (VM26) from Bristol-Myers Squibb Australia; Taxol from Calbiochem; mafosfamide from ASTA MEDICA; methotrexate from David Bull Laboratories; geneticin (G418) from Life Technology; Alamar blue reagent from Astral Scientific; verapamil from Sigma Aldrich; Lipofectamine 2000 from Invitrogen Life Technologies; puromycin, polybrene, crystal violet, and methylene blue from Sigma-Aldrich.

The following monoclonal antibodies were used: anti-human p53 (DO-1, Santa Cruz Biotechnology), anti-human p21 (clone SX118, PharMingen), anti-human MRP1 (Alexis Biochemicals), anti-human P-glycoprotein (clone C219, DAKO Corporation), anti-actin (Sigma-Aldrich), and anti–glyceraldehyde-3-phosphate dehydrogenase (GAPDH; clone 6C5, Abcam Ltd.). Polyclonal anti-human Bax antibody is from BD PharMingen.

Short-term cytotoxicity assays and clonogenic assay. Response of cells to chemotherapeutic drugs was determined using either a 72-h Alamar blue assay or a 24-h methylene blue assay as previously described (18, 19). For clonogenicity assay, cells were seeded at 100 per well in six-well plates and treated with increasing concentrations of cisplatin (24 h), doxorubicin, vincristine, and VM26 (72 h), respectively, then cultured in drug-free medium for 8 to 10 days until colonies formed to reasonable size. Cells were fixed with methanol and stained with crystal violet (0.5% crystal violet in water with 50% methanol). Colonies containing >50 cells were counted. Plating efficiency was defined as the number of colonies observed from the untreated cells divided by the number of cells plated. Surviving fraction was determined by dividing the colonies counted by the number of cells seeded with a correction for plating efficiency.

Reverse transcription-PCR analysis. The semiquantitative reverse transcription-PCR (RT-PCR) protocols involving coamplification of the target gene sequence and a control gene sequence (*β_2-microglobulin*) in the same reaction have been described previously (12, 20). The gene-specific primers used for MDR1, MRP1, and β_2-microglobulin have been described previously (12). The other primers used were as follows. MRP2 (forward 5′-ACCAATCCAAGCCTCTACCTAG-3′, reverse 5′-GAAAGTGCCA-CAGAGTATCGAG-3′), MRP3 (forward 5′-GCTTTCTCTCCCGCCTGTT-3′, reverse 5′-TTTAGGGACCAGAGGTCCTTCTC-3′), GST-π (forward 5′-GGACCTCCGCTGCAAATAC-3′, reverse 5′-GAAGGTCTTGCCTCCCTGG-3′), γGCS (forward 5′-CTACGGAGGAACAATGTCCGA-3′, reverse 5′-CCCAGGA-CAGCCTAATCTGG-3′), and metallothionein (forward 5′-CYGGTGDCT-CCTGCACCTG-3′, reverse 5′-CCCCTTTGCAGAYRCAGYC-3′).

Microarray analysis. Total cytoplasmic RNA was extracted from IMR-32 and IMR/KAT100 cells using RNA extraction kit RNeasy (Qiagen). cDNA microarrays containing 4,000 genes on glass slides were done by Peter MacCallum Cancer Institute (Melbourne, Australia). In a first experiment, RNA isolated from IMR-32 cells served as the reference cDNA for IMR/KAT100 cells, with an aim to identify genetic changes due to drug selection that conferred MDR in IMR/KAT cells. In a second experiment, IMR-32 and IMR/KAT100 cells were treated with 2, 20, and 200 μmol/L VP-16 or with 1 and 5 Gy γ-irradiation separately. cDNA from treated cells and untreated control cells were competitively hybridized to the reference cDNA on the microarray slides. The responses of the IMR-32 parental cells and IMR/KAT cells to the treatments were compared to identify candidate genes that were responsible for the MDR in IMR/KAT100 cells. Microarray data were analyzed using GeneSpring software (version 4.1.5, Silicon Genetics).

***p53* gene sequencing.** The entire p53 coding region (exons 2–11) was amplified by PCR using Human p53 Amplimer Panels (Clontech Laboratories, Inc.). The PCR products were gel purified and sequenced in both directions using automated fluorescence-based cycle sequencing with BigDye terminators (PE Biosystems). p53 sequences were compared with the wild-type sequence deposited in Genbank (accession nos. X54156 and U94788) using AssemblyLIGN computer software (Oxford Molecular Group).

Construction of mutant p53 expression vectors and transfection. Site-directed mutagenesis was done to generate vectors expressing p53 protein with a codon 135 mutation (M135), using the GeneEditor *in vitro* Site-Directed Mutagenesis System (Promega) according to the manufacturer's instructions. A mutagenic oligonucleotide (5′-AAGATGTTTTTC-CAACTGGC-3′) was designed for generating the p53 codon 135 mutation in the pCMV-*Neo* vector containing wild-type p53 cDNA sequence, which was kindly provided by Dr. B. Vogelstein (John Hopkins University, Baltimore, MD). The presence of p53 M135 mutation in the resultant plasmid was determined by sequencing the full-length p53 cDNA. Human neuroblastoma SH-EP cells were transfected with the mutant p53 constructs and pCMV-Neo vector-only, respectively, using calcium phosphate transfection methods (21). Cells were selected with geneticin (G418) and single clones were analyzed by Western blot for expression of mutant p53 protein.

Retroviral transductions. Two retroviral constructs were used to inactivate p53 in transduced cells: one is modified pBabe vector containing p53 short hairpin RNA (shRNA), the other one is pLXSP vector containing dominant-negative p53 mutant encoding truncated protein corresponding to COOH-terminal fragment of p53 (GSE56), both of which specifically abrogate wild-type p53 function (22). We generated stable p53-deficient variants from a panel of p53 wild-type tumor cell lines of neuroblastoma (IMR-32, SK-N-SH, SH-EP, and SH-SY5Y) and nonneuroblastoma origin (RCC26b, RCC45, RCC54, ACHN, U2OS, HT1080, MCF7, and LNCaP) using standard retroviral transduction protocol.

Western analysis. To analyze the expression of MRP1 and MDR1 proteins, crude membranes were prepared (23) and Western blot analysis was done as described previously (24). Following incubation with the appropriate dilution of primary antibody (p53, 1:3,000–1:5,000; p21, 1:500; Bax, 1:2,000; MRP1, 1:500; P-glycoprotein, 1:200; actin, 1:2,000; GAPDH, 1:20,000) for 2 to 4 h, membranes were washed and then incubated with an appropriate horseradish peroxidase–conjugated secondary antibody for 1 to 2 h. Binding of the secondary antibody was detected by SuperSignal (Pierce Biotechnology).

Irradiation and cell cycle analysis. Irradiation was done using a ^{137}Cs γ-irradiator (model 143-45A, J.L. Shepherd and Associates). For cell cycle analysis, early log-phase cells were either treated with doxorubicin at various concentrations for 24 h, or exposed to different dosages of γ-irradiation. At designated time points, floating cells were collected by centrifugation, combined with trypsinized attached cells, and fixed with ice-cold 70% ethanol for at least 1 h before incubation at 37°C (30 min) in staining solution consisting of propidium iodide (50 μg/mL) and RNase (2 μg/mL) in PBS. Stained cells were analyzed for DNA content on a FACSCalibur flow cytometer (Becton Dickinson) using CELL Quest analysis software (Becton Dickinson).

Senescence-associated β-galactosidase staining. For senescence-associated β-galactosidase activity, cells were fixed and stained at pH 6.0 with 5-bromo-4-chloro-3-indol β-D-galactopyranoside (X-gal) as described (25).

Statistical analysis. Statistical analyses were done using StatView (version 5.0.1; SAS Institute, Inc.). For cytotoxicity assay, determination of ID_{50} values and statistical analysis were done as described previously (26).

Results and Discussion

Isolation and properties of a MDR human neuroblastoma cell line IMR/KAT100. The IMR/KAT100 line was selected as a result of repeated 3-day exposure of parental IMR-32 human neuroblastoma cells to stepwise increases of the heavy metal compound, KAT. The drug resistance profile for both parental IMR-32 cells and IMR/KAT100 cells in 72-h cytotoxicity assays is shown in Fig. 1*A*. By comparison with the parental IMR-32 cells, IMR/KAT100 cells displayed 5-fold resistance to the selecting drug, KAT. In addition, however, these cells also showed significantly increased resistance to a range of structurally unrelated drugs, including the anthracyclines doxorubicin and daunorubicin, the *Vinca* alkaloid vincristine, the epipodophyllotoxins etoposide and teniposide, the alkylating agents melphalan and mafosfamide, and the platinum compound cisplatin. No significant increase in resistance to either the antifolate methotrexate or the microtubule-stabilizing agent

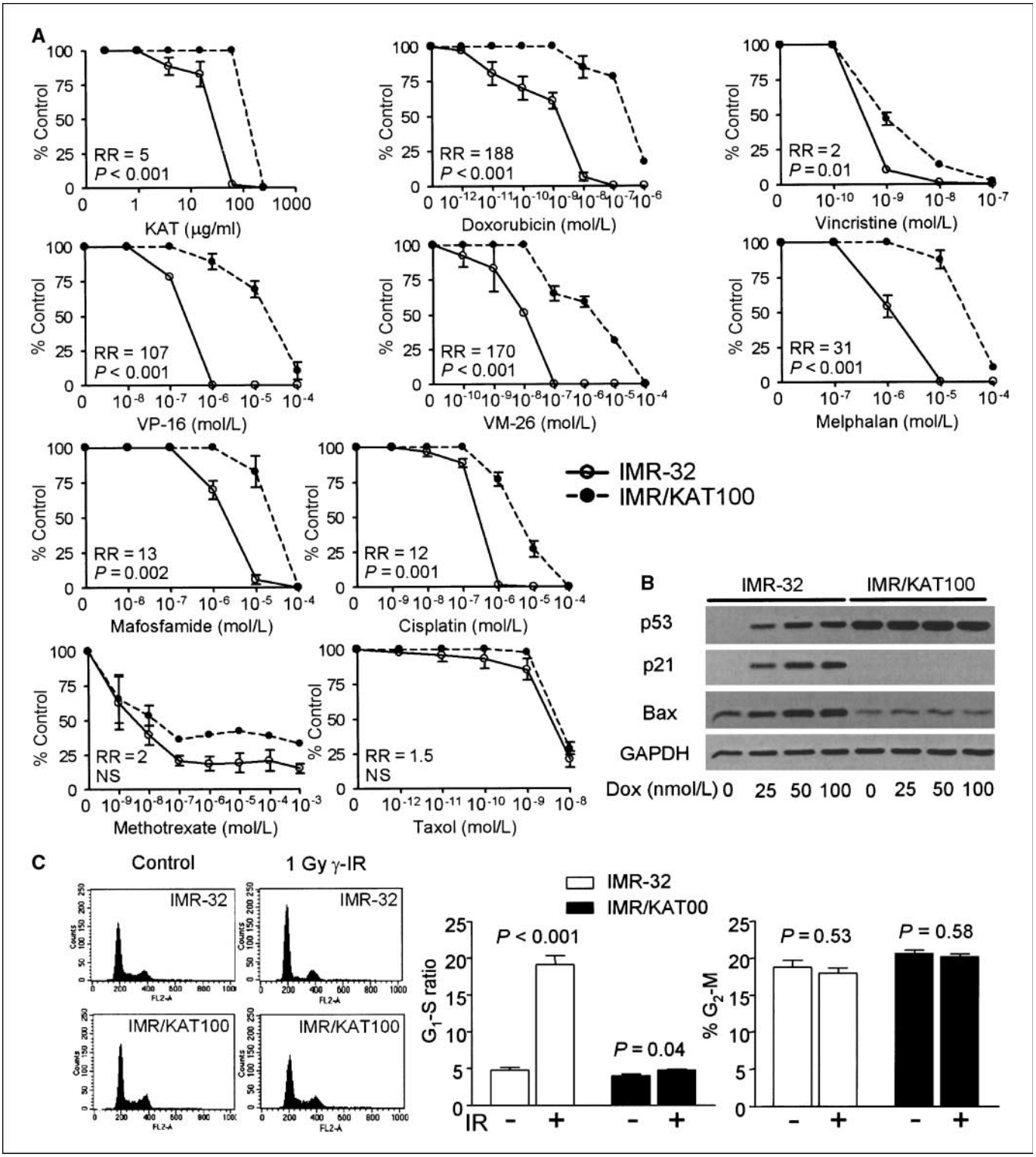

Figure 1. *A,* cross-resistance profile of drug-selected neuroblastoma cells. Response of IMR/KAT100 and parental IMR-32 cells to a range of chemotherapeutic drugs after a 72-h Alamar blue assay. *Points,* mean of at least three independent runs; *bars,* SE. *RR,* relative resistance. *NS,* not significant. *B,* Western blot analysis demonstrating lack of induction of p53, p21, and Bax in IMR/KAT100 after doxorubicin (*Dox*) treatment. *C,* cell cycle analysis of IMR-32 and IMR/KAT100 cells 24 h after γ-irradiation (*IR*). Histogram shows DNA content in each phase of cell cycle. *Columns,* change in G_1-S ratio and the percentage of cells in G_2-M phase; *bars,* SE.

Taxol was observed. A similar pattern of cross-resistance was observed in 24-h cytotoxicity assays (data not shown).

The trivalent antimonial compound KAT has been shown to be substrate for the MRP1 transporter, and we have provided strong evidence that *MRP1* expression is a powerful independent marker of outcome in the treatment of this disease (12, 13). To investigate the mechanisms underlying drug resistance in the IMR/KAT100 cells, we therefore examined the expression of a

number of well-characterized genes, associated with a MDR phenotype, including *MDR1, MRP1-3, GST-π, γGCS*, and *metallothionein*. Following RT-PCR analysis, no increased expression of any of these genes was observed, whereas Western blot analysis showed no detectable change in either MDR1 or MRP1 protein levels in the IMR/KAT100 cells by comparison with the parental IMR-32 cells (data not shown).

To identify possible genetic changes responsible for the unusual MDR phenotype observed, cDNA microarray analysis was done, after treatment of the parental and drug-resistant cells, with varying doses of VP-16 or γ-irradiation. Microarray data from two independent experiments confirmed the lack of involvement of well-characterized MDR-associated genes (data not shown). However, IMR/KAT100 cells showed a lack of induction of four p53-regulated genes, *p21* (*$p21^{WAF1}$*), *BTG2, WIP1*, and *p48*, by comparison with the up-regulation of these genes in the parental IMR-32 cells. This defective p53 pathway was confirmed by Western blot analyses in which a dose-dependent induction of p21 and Bax was observed in IMR-32 parental cells, but not in IMR/KAT100 cells, after treatment with different concentrations of doxorubicin (Fig. 1*B*). We also examined p53-mediated control of cell cycle checkpoints using fluorescence-activated cell sorting analysis of cell distribution among the phases of the cell cycle after low-dosage γ-irradiation. Although IMR-32 cells underwent strong G_1-S arrest, as shown by the DNA histogram at 24 h postirradiation, IMR/KAT100 cells failed to display significant G_1-S cell cycle arrest (Fig. 1*C*).

The entire coding region of *p53* gene was sequenced in the IMR/KAT100 cells and a point mutation was identified at codon 135 (exon 5) within the DNA-binding domain (G-T transversion), leading to an amino acid change from cysteine to phenylalanine. This mutation (M135) was accompanied by loss of heterozygosity, as shown by a change of a codon 72 polymorphism from CCC/CGC to CGC. Interestingly, an identical mutation at codon 135 has also been previously reported in another human neuroblastoma cell line [SK-N-BE(2c)] established from a patient with relapsed disease (27). In addition, another study observed that exposure of a *MYCN*-amplified neuroblastoma cell line (UKF-NB-3) to increasing concentrations of vincristine resulted in the generation of a highly drug-resistant subline (UKF-NB-3^{r}VCR^{10}), and although this subline exhibited high levels of P-glycoprotein–mediated MDR, it had also acquired the exact p53 mutation (M135phe) as observed in the IMR/KAT100 cells (28). Thus, these observations pointed at p53 pathway deregulation as a potential mechanism for alterations in the drug sensitivity observed.

To investigate the functionality of the p53 pathway in neuroblastoma cells, we stably transduced SK-N-SH, SH-EP, and SH-SY5Y neuroblastoma cells with the constructs expressing shRNAs against p53 or GFP (negative control), and investigated the p53 transactivation activity in these cells in response to DNA damage. As shown in Fig. 2*A*, after doxorubicin treatment, the control cells of all three cell lines (SK-N-SH/shGFP, SH-EP/shGFP, and SH-SY5Y/shGFP) displayed strong dose-dependent induction of p53, as well as p21 and Bax encoded by p53-responsive genes. In contrast, knocking down p53 in these cells by shRNA (SK-N-SH/shp53, SH-EP/shp53, and SH-SY5Y/shp53) resulted in a loss of p21 induction, and lack of induction (SK-N-SH/shp53 and SH-SY5Y/shp53) or reduced induction of Bax (SH-EP/shp53). Together, these results show that p53 is functional and able to transcriptionally activate target genes in a range of neuroblastoma cells.

Mutant p53 can confer a MDR phenotype into other neuroblastoma cells. To determine whether the acquisition of the p53 mutation was responsible for the MDR phenotype of the IMR/KAT100 cells, p53 wild-type human SH-EP cells were transfected with a p53 M135 construct, pCMV-M135, generated using site-directed mutagenesis. Following transfection, multiple clones were isolated, and four were selected for further analysis. Both these clones expressed high levels of mutant p53 protein (Fig. 2*B*).

The SH-EP M135 transfectants failed to induce any significant levels of p21 expression after doxorubicin treatment (Fig. 2*B*). This contrasted with the vector controls, SH-EP/CMV1 and SH-EP/CMV2, both of which strongly induced p53 and p21 after drug treatment (Fig. 2*B*). Lack of p21 and Bax induction was also observed in the mutant clones after treatment with γ-irradiation (data not shown). Furthermore, by comparison with the vector controls, cell cycle analysis on these mutant transfectants showed a failure of any significant G_1-S cell cycle arrest, 24 h after γ-irradiation compared with control cells (Fig. 2*C*). Thus, M135 mutant p53 confers a dominant-negative phenotype.

To address the key question of whether the p53 M135 mutation is able to confer a MDR phenotype in the transfectant SH-EP cells, we conducted 72-h cytotoxicity assays to a range of cytotoxic drugs that had similarly been tested in IMR/KAT100 cells (Table 1). By comparison with the vector controls, the p53 M135-transfected clones showed significant resistance to doxorubicin (3.7-fold), VM26 (11.5-fold), cisplatin (2.2-fold), and vincristine (4.1-fold). In addition, the mutant clones showed 2.4-fold resistance to KAT, the drug used for selection of the IMR/KAT100 cells. However, none of the mutant clones exhibited any significant change in response to either Taxol or methotrexate, drugs to which the IMR/KAT100 cells were also not resistant.

The results of these short-term cytotoxicity assays also correlated with the outcome of clonogenic assays, in which the empty vector controls showed a stronger dose-dependent decline in the number of colony-forming cells compared with cultures expressing mutant p53. The mutant clones showed increased resistance to cisplatin (2.5-fold), vincristine (1.5-fold), VM26 (1.5-fold), and doxorubicin (1.4-fold; Table 2). However, the scale of drug resistance gained by M135-expressing cell lines was smaller than that of the short-term cytotoxicity assays, suggesting that a significant fraction of the M135-expressing cells that survived 72-h treatment were incapable of long-term proliferation. Taken together, these results suggest that p53 status may be an important marker of treatment response in neuroblastoma, and in this regard provide support for a previous study by Layfield et al. (29), showing p53 staining in primary neuroblastoma tumor samples to be a prognostic of outcome.

p53 M135 mutant–mediated MDR results from its p53-suppressive rather than gain-of-function activity. In some tumor types, gain of function is believed to be mechanism by which mutant p53 contributes to tumor progression and an increase in cellular resistance to chemotherapy and ionizing radiation (30). We tested the possibility of mutant p53 causing up-regulation of drug resistance genes in SH-EP cells but found no changes in the expression of MRP1 or MDR1 at either the gene or protein level (data not shown). Therefore, to determine whether the drug-resistant phenotype resulted from loss of wild-type p53 function or gain of mutant function, we compared the drug resistance of M135-expressing cells with similar cells, in which p53 function was suppressed by either shRNA or GSE56. GSE56 is a suppressing element that encodes a fragment of p53 acting as a potent

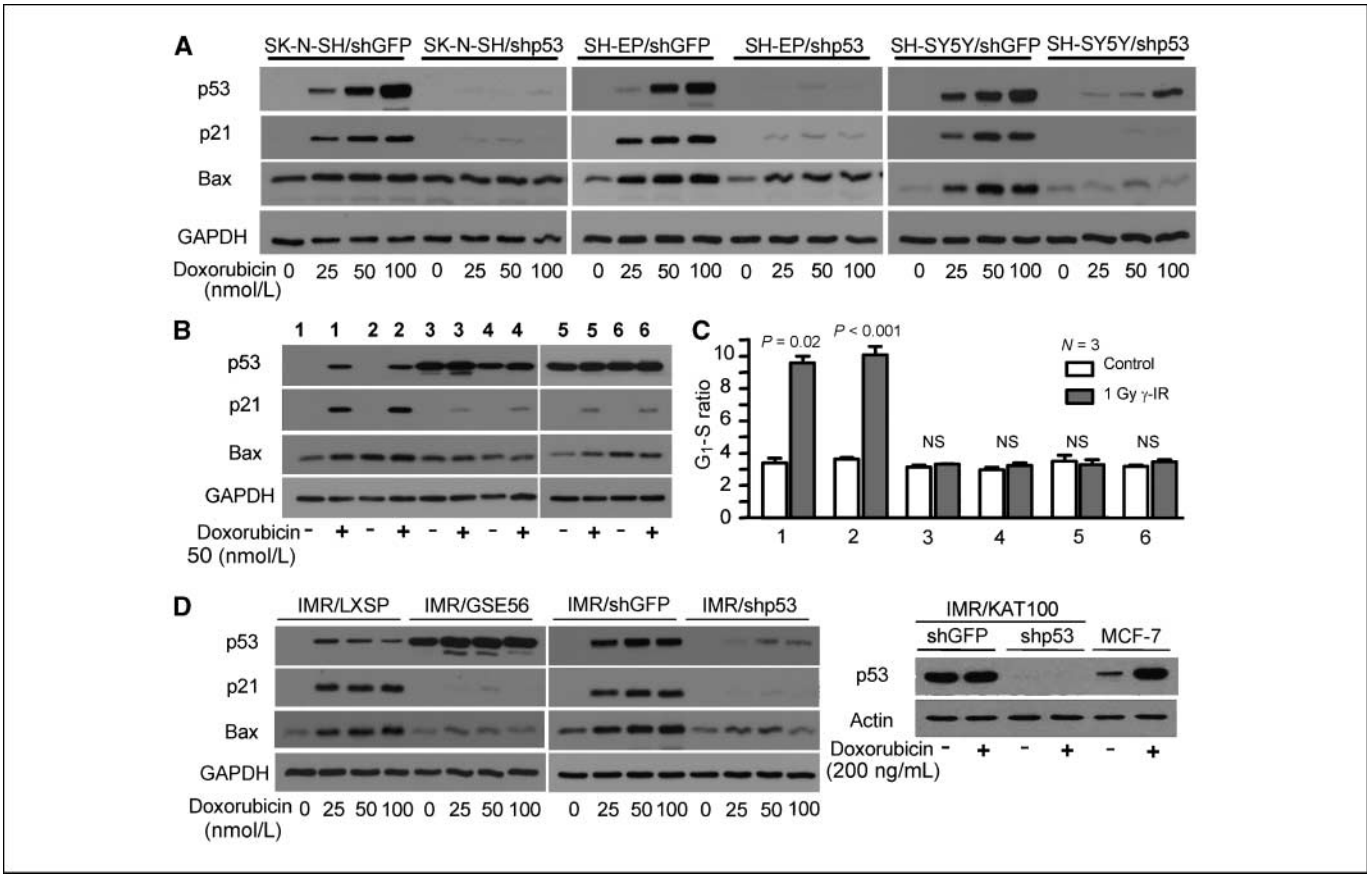

Figure 2. *A,* Western analysis of p53 and its target genes in shRNA-transduced neuroblastoma cells. SK-N-SH, SH-EP, and SH-SY5Y cells were treated with three different concentrations (25, 50, and 100 nmol/L) of doxorubicin for 24 h, before analysis of p53, p21, and Bax. GAPDH was used as a loading control. *shp53,* transduced cells expressing shRNA specific for p53; *shGFP,* transduced cells expressing shRNA for control GFP. *B,* Western blot analysis of expression of p53 and its target genes in SH-EP cells transfected with mutant p53 (M135) after drug treatment. *Lanes 1* and *2,* empty vector controls SH-EP/CMV1 and SH-EP/CMV2; *lanes 3* to *6,* four mutant clones SH-EP/M135-1, SH-EP/M135-2, SH-EP/M135-3, and SH-EP/M135-4. *C,* cell cycle analysis of p53 M135 SH-EP transfectants 24 h after 1 Gy γ-irradiation. *Columns,* comparison of the changes in G_1-S ratios before and after irradiation; *bars,* SE. Vector controls (*1* and *2*) underwent significant G_1-S arrest, compared with the four mutant clones (*3–6*) that failed to do so. *D,* Western blot analysis of expression of p53 and its target genes *p21* and *Bax* 12 h posttreatment with doxorubicin in transduced IMR-32 and IMR/KAT-100 cells expressing either GSE56 or shRNA against p53. IMR/LXSP and IMR/shGFP (shRNA against GFP) were used as controls for the transduced cells, respectively. GAPDH and actin were used as loading controls. MCF7 was used as a control for functional p53.

dominant-negative mutant (31). By comparison with the vector controls (IMR/LXSP and IMR/shGFP), both GSE56- and shRNA-transduced IMR-32 cells (IMR/GSE56 and IMR/shp53) showed reduced induction of p53-regulated genes *p21* and *Bax* after doxorubicin treatment (Fig. 2*D*) and increased resistance to a range of chemotherapy drugs with different modes of action (Table 3). Interestingly, inhibiting wild-type p53 function by either p53 GSE56 or by shRNA did not significantly change the sensitivity of IMR-32 cells to Taxol. Thus, the pattern of cross-resistance observed in neuroblastoma cells with loss of wild-type p53 mirrors that displayed by the IMR/KAT100 cells.

We abrogated expression of the mutant protein in IMR/KAT100 cells by stably expressing shRNA against p53 using retroviral transfer. By comparison with control cells transduced with shRNA against GFP (IMR/KAT100/shGFP), p53 was barely detectable in the IMR/KAT100 cells transduced with shRNA against p53 (IMR/KAT100/shp53), either before or after doxorubicin treatment (Fig. 2*D*). Cytotoxicity assays showed that IMR/KAT100/shp53 cells were not sensitized to a range of drugs, including cisplatin, doxorubicin, vincristine, and VM26, by comparison with the control IMR/KAT100/shGFP cells (Table 3), indicating that gain of function of mutant p53 is not a mechanism of MDR in the IMR/KAT100 cells. Taken together, the above data strongly suggest that it is the loss of wild-type p53 function that contributes to the MDR phenotype in neuroblastoma cells. A previous study, conducted by Keshelava et al. (14), provided initial evidence that defective p53 function confers MDR in neuroblastoma cell lines. However, inactivation of wild-type p53 in this study was achieved by transfection of cells with HPV16 E6 and a number of reports have shown that the E6 protein has effects other than targeting p53 (32) and is not equivalent to that of a mutant p53 or a knockout of p53 (33). In contrast to this study, we used highly specific RNA interference technology and GSEs to silence p53 to generate pairs of neuroblastoma cell lines with either functional or inactivated p53. These isogenic pairs of lines have uniquely shown that loss of functional p53 led to decreased sensitivity to a number of clinically used drugs. Our results thus provide definitive evidence of a role for p53 as a drug sensitivity gene in neuroblastoma.

The lack of an effect of p53 status on cellular response to Taxol is in agreement with previous studies (34, 35) and contrasts with the increased resistance observed to the microtubule-destabilizing drug vincristine. Although Taxol and vincristine are both antimicrotubule

Table 1. Response of p53 M135 SH-EP transfectants to cytotoxic drugs in 72-h cytotoxicity assays

Drug	Cell line	ID_{50}		Fold resistance*	P †
KAT	SHEP/CMV	6.731 ± 1.115 μg/mL			
	SHEP/M135	15.943 ± 1.834 μg/mL		2.37	0.023
		Log (drug) ± SE ‡	M§		
Doxorubicin	SHEP/CMV	−7.690 ± 0.050	2.042×10^{-8}		
	SHEP/M135	−7.119 ± 0.056	7.603×10^{-8}	3.72	<0.001
Vincristine	SHEP/CMV	−9.163 ± 0.028	6.87×10^{-10}		
	SHEP/M135	−8.550 ± 0.035	2.82×10^{-9}	4.10	<0.001
VM26	SHEP/CMV	−6.987 ± 0.083	1.03×10^{-7}		
	SHEP/M135	−5.928 ± 0.107	1.18×10^{-6}	11.46	<0.001
Cisplatin	SHEP/CMV	−5.851 ± 0.030	1.41×10^{-6}		
	SHEP/M135	−5.517 ± 0.037	3.04×10^{-6}	2.16	<0.001
Methotrexate	SHEP/CMV	−7.834 ± 0.092	1.47×10^{-8}		
	SHEP/M135	−7.564 ± 0.101	2.73×10^{-8}	1.86	NS
Taxol	SHEP/CMV	−8.261 ± 0.061	5.48×10^{-9}		
	SHEP/M135	−8.166 ± 0.046	6.82×10^{-9}	1.24	NS

Abbreviation: NS, not significant.
*The fold resistance was determined by dividing the ID_{50} of the p53 M135–transfected SH-EP cells by that of the vector control SH-EP/CMV cells.
† For a given drug, P values were determined by comparing the ID_{50} value for the p53 M135–transfected SH-EP cells with the ID_{50} value of the control SH-EP/CMV cells assayed in the same series of experiments.
‡ Calculated from at least three replicate assays.
§Molar concentration.

agents, their mechanisms of action are quite distinct. Thus, Taxol acts by inducing polymerization of microtubules whereas vincristine acts as a microtubule-depolymerizing drug. Previous studies have shown that p53 localizes to cellular microtubules and that treatment with vincristine or Taxol leads to a reduction in the nuclear accumulation of p53 (36). However, there have also been a number of reports in the literature that drug response of cancer cells to Taxol, unlike vincristine, appears to be independent of p53 status. For example, data from a large-scale drug screening project using 60 different cancer cell lines conducted by National Cancer Institute showed that response of cells to Taxol did not have a clear correlation with p53 status (34). One possible explanation for this differential effect after treatment with these two drugs may relate to the increased expression of the microtubule-stabilizing protein MAP4, which has been shown to occur in cells with dysfunctional p53 (37). Understanding the mechanism of MDR associated with loss of p53 function in neuroblastoma suggests that Taxol should be more effective in killing cells undergoing mitotic catastrophe than other chemotherapeutic drugs. However, this prediction remains to be experimentally tested.

Mechanism of p53-mediated drug response of neuroblastoma cells. To determine mechanism(s) underlying p53 dependence of drug sensitivity of neuroblastoma cells, we measured distribution

Table 2. Response of p53 M135 SH-EP transfectants to cytotoxic drugs in clonogenic assays

Drug	Cell line	ID_{50}*	Fold resistance †	P ‡
Doxorubicin	SHEP/CMV	4.420 ± 0.092		
	SHEP/M135	6.202 ± 0.181	1.40	<0.001
Vincristine	SHEP/CMV	0.608 ± 0.011		
	SHEP/M135	0.899 ± 0.031	1.48	<0.001
VM26	SHEP/CMV	20.328 ± 1.298		
	SHEP/M135	29.438 ± 0.804	1.45	<0.001
Cisplatin	SHEP/CMV	0.315 ± 0.024 μmol/L		
	SHEP/M135	0.801 ± 0.060 μmol/L	2.54	<0.001

*Calculated from at least three replicate assays.
† Fold resistance was determined by dividing the ID_{50} of the p53 M135–transfected SH-EP cells by that of the control SH-EP/CMV cells.
‡ For a given drug, P values were determined by comparing the ID_{50} value for the p53 M135–transfected SH-EP cells with the ID_{50} value of the control SH-EP/CMV cells assayed in the same series of experiments.

Table 3. Response of transduced IMR-32 and IMR/KAT100 cells to cytotoxic drugs in 72-h cytotoxicity assays

Drug	Cell line	Fold resistance*	P †	Cell line	Fold resistance*	P †	Cell line	Fold sensitization ‡	P§
Doxorubicin	IMR/LXSP			IMR/shGFP			IMR/KAT100/shGFP		
	IMR/GSE56	2.46	0.045	IMR/shp53	3.10	0.004	IMR/KAT100/shp53	0.57	NS
Vincristine	IMR/LXSP			IMR/shGFP			IMR/KAT100/shGFP		
	IMR/GSE56	1.64	0.039	IMR/shp53	3.62	0.036	IMR/KAT100/shp53	0.85	NS
VM26	IMR/LXSP			IMR/shGFP			IMR/KAT100/shGFP		
	IMR/GSE56	1.63	0.013	IMR/shp53	1.51	0.002	IMR/KAT100/shp53	0.13	NS
Cisplatin	IMR/LXSP			IMR/shGFP			IMR/KAT100/shGFP		
	IMR/GSE56	3.92	0.001	IMR/shp53	3.01	0.004	IMR/KAT100/shp53	0.45	NS
KAT	IMR/LXSP			IMR/shGFP					
	IMR/GSE56	1.29	0.024	IMR/shp53	1.31	0.024			
Melphalan	IMR/LXSP			IMR/shGFP					
	IMR/GSE56	20.19	<0.001	IMR/shp53	—	—			
Taxol	IMR/LXSP			IMR/shGFP					
	IMR/GSE56	2.29	NS	IMR/shp53	1.72	NS			

*The fold resistance was determined by dividing the ID_{50} of IMR/GSE56 or IMR/shp53 cells by that of control IMR/LXSP or IMR/shGFP cells, respectively.

† For a given drug, P values were determined by comparing the ID_{50} value for IMR/GSE56 or IMR/shp53 cells with the ID_{50} value of their corresponding control cells assayed in the same series of experiments.

‡ The fold sensitization was calculated by dividing the mean ID_{50} for the control IMR/KAT100/shGFP cells by the mean ID_{50} for the IMR/KAT100/shp53 cells.

§For a given drug, P valves were determined by comparing the ID_{50} value for IMR/KAT100/shGFP cells with the ID_{50} value of IMR/KAT100/shp53 cells assayed in the same series of experiments.

of cells among phases of the cell cycle in cultures of isogenic populations of neuroblastoma cell lines differing in their p53 function after genotoxic stress. Representative results of these analyses are shown in Fig. 3(*A–C*). Doxorubicin- and radiation-induced growth arrest in both types of cells is seen 24 h post-treatment as almost complete lack of cells in S-phase (Fig. 3*A* and *B*). This arrest appeared to be permanent for p53 wild-type cells, the majority of which stayed on the plates during the whole duration of the experiment (2 weeks; Fig. 3*C*). Arrested p53 wild-type cells expressed acidic β-galactosidase, a marker of cellular senescence (ref. 25; Fig. 3*C*). In contrast, however, in p53-deficient cells after DNA damage, growth arrest was either temporary (as judged by reappearance of S-phase) or incomplete. Resumption of cell cycle progression was accompanied by gradual accumulation of cells with both sub-G_1 and polyploid (>4C) DNA content (Fig. 3*A* and *B*). Simultaneously, numerous multinucleated cells and cells with multiple micronuclei appeared (data not shown) and the population underwent significant cell loss: By the end of the period of observation, most parts of the plate surface contained no cells (Fig. 3*C*). At the same time, in treated populations of p53-deficient cells, we observed formation of multiple colonies of rapidly dividing cells with no traces of senescence-specific β-galactosidase (Fig. 3*C*). The frequency of such colonies inversely correlated with the dose of treatment.

The results above indicate that the majority of cells, regardless of their p53 status, lose the capability to proliferate after DNA damage. However, the mechanism of such loss is very different in p53 wild-type and deficient cells. The major type of DNA damage response of the p53 wild-type neuroblastoma cells is irreversible growth arrest (senescence) that may occur both in G_1 and G_2 phases of the cell cycle. However, cells deficient in p53 instead attempt to proceed through the cell cycle but fail to complete cytokinesis and become polyploid with DNA segregated among multiple nuclei, typical signs of mitotic catastrophe, followed by apoptotic death (appearance of sub-G_1 fraction). Hence, p53 prevents neuroblastoma cells from lethal mitotic catastrophe but brings them into senescence so effectively that it is interpreted by drug assays as a high degree of drug sensitivity. Although the majority of cells in p53-deficient variants of this line die from mitotic catastrophe and apoptosis, this mechanism of cell killing is less efficient than p53-mediated senescence in p53 wild-type variant and is interpreted as drug resistance. These data therefore suggest that lack of p53 does not make each individual cell more resistant to DNA damage but rather allows rare survivors to continue to proliferate.

A number of previous studies have shown a defective DNA damage–induced G_1 checkpoint in neuroblastoma cells with wild-type p53 despite p21 induction (38, 39). These data, which were obtained using relatively high doses of γ-irradiation, do not support a fully functional p53 pathway in this tumor type because G_1 checkpoint control is one of the most critical functions of p53 as a tumor suppressor. In contrast to these investigations, we found marked G_1 arrest in neuroblastoma cells without significant change in the G_2 population after treatment with low dosages of γ-radiation. These changes in cell cycle were not observed in neuroblastoma cells with mutant p53. At higher dosages of irradiation, N-type IMR-32 cells underwent apoptosis rather than cell cycle arrest (data not shown) whereas S-type SH-EP cells underwent senescence. Similar results were also observed in these cells after treatment with various dosages of doxorubicin. Thus, this study shows that the cellular response of wild-type p53 neuroblastoma cells after DNA damage is largely dependent on the extent of DNA damage and cell type. Our data therefore provide strong evidence for a fully functional p53 pathway in G_1 checkpoint

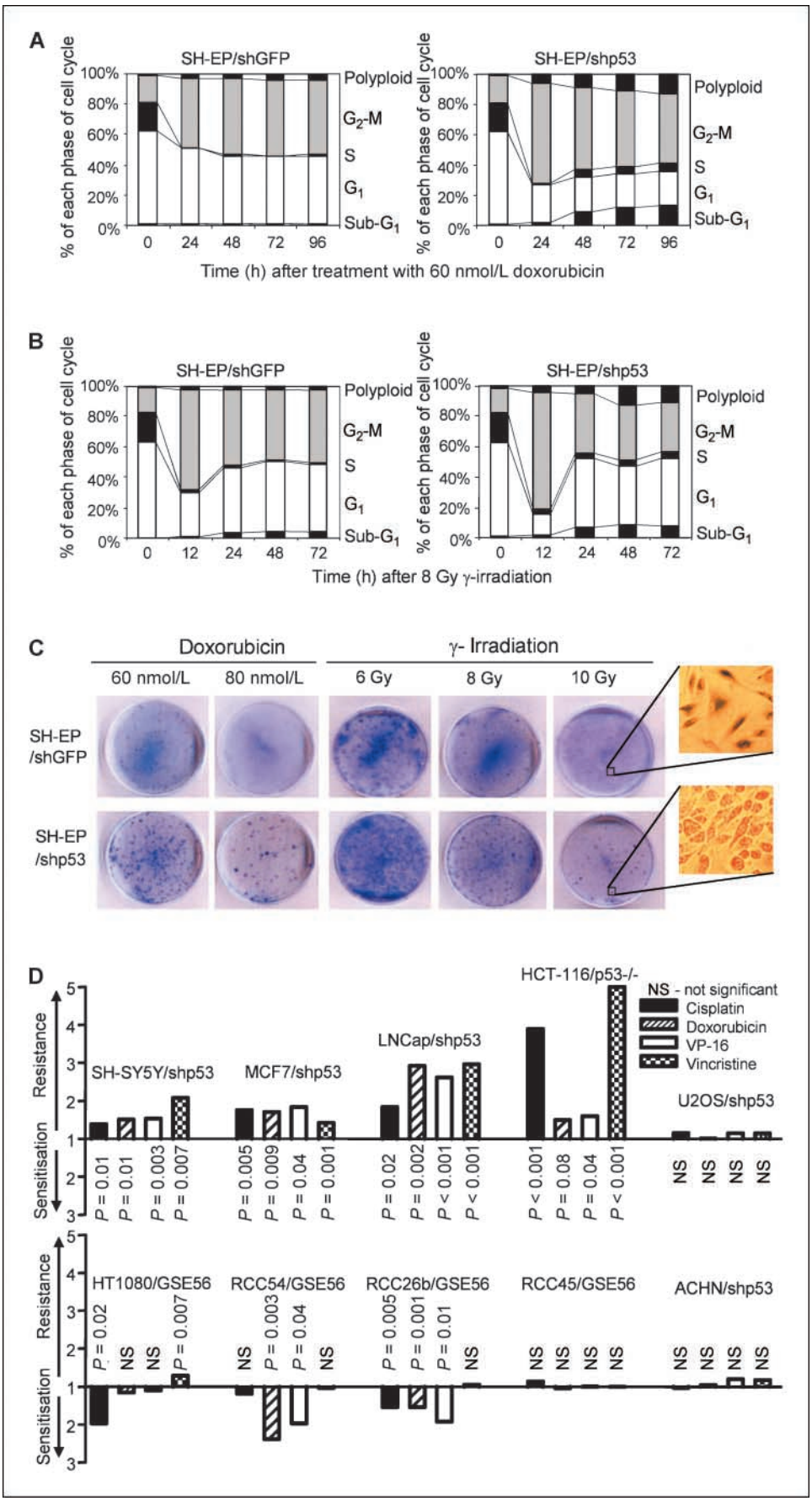

Figure 3. *A* and *B,* distribution of cells among phases of the cell cycle in cultures of p53 siRNA-transduced human neuroblastoma SH-EP cells after treatment by either doxorubicin (*A*) or γ-irradiation (*B*). Cellular DNA content was measured at various times before and after treatment. *C,* p53 shRNA-transduced human neuroblastoma SH-EP cells at 2 wk after treatment with doxorubicin or γ-irradiation. These cultures were then stained with crystal violet for visualizing proliferating cells. The frequency of colonies inversely correlated with the dose of treatment. β-Galactosidase staining (at pH 6.0) is shown to the right. *D,* effect of p53 status on response of nonneuroblastoma cells to cytotoxic drugs. Response of neuroblastoma cell line SH-SY5Y and nine pairs of nonneuroblastoma cell lines differing in their p53 status to chemotherapeutic drugs measured using a 24-h short-term cytotoxicity assay. A pair of colon carcinoma cell lines, HCT-116/p53−/− with deletion of p53 and parental HCT-116 cells with wild-type p53, was also included. The plot shows the mean of sensitivity (based on ID_{50}) of each p53-deficient cell line to each drug by comparison with its p53 wild-type counterpart from three independent experiments.

control, and the finding of treatment-induced senescence in wild-type p53 neuroblastoma cells provides further evidence of this functionality.

***p53* is not always a drug sensitivity gene: comparison of neuroblastoma with other cancer cell types.** To investigate the role of p53 in determining drug response in other cell types, we generated p53-deficient variants from a panel of p53 wild-type tumor cell lines of nonneuroblastoma origin. The cell lines investigated included renal carcinoma (RCC26b, RCC45, RCC54, and ACHN), osteosarcoma (U2OS), lung fibrosarcoma (HT1080), breast cancer (MCF7), and prostate cancer (LNCaP). In addition, the colon carcinoma cell line, HCT-116, as well as its p53-deficient variant HCT-116/p53−/−, were also studied. Knockdown of p53 was achieved by transduction of p53-suppressive constructs encoding either shRNA or the dominant-negative p53 mutant, p53GSE56. All of these p53-deficient variants displayed dramatic reduction of p21 and Bax induction after doxorubicin treatment compared with the control cell lines (data not shown).

The response of these isogenic pairs of tumor cell lines to chemotherapeutic drugs was measured by short-term cytotoxicity assays, and the results are shown in Fig. 3*D*. Similar to the results above with the neuroblastoma cell lines, p53 suppression conferred a drug resistance phenotype in breast cancer, prostate cancer, and colon carcinoma, whereas no effect or increased drug sensitivity was observed in renal cell carcinoma, osteosarcoma, and lung fibrosarcoma.

p53 alterations have been linked to the failure of radiotherapy and chemotherapy in a variety of cancers both *in vitro* and *in vivo* (40, 41). In hematologic malignancies, p53 mutations are less frequent but a strong correlation was found to be associated with unfavorable prognostic factors and resistance to chemotherapy (41, 42). Likewise, p53 mutations in breast cancer have been associated with resistance to tamoxifen, doxorubicin, and radiotherapy (41, 43), whereas similar mutations in ovarian cancer patients were found to be significantly correlated with resistance to platinum-based chemotherapy, early relapse, and shortened overall survival (44). However, clinical data are also emerging to support both positive and negative correlations between p53 mutations and drug sensitivity of tumors. For example, p53 mutations have been correlated with increased drug sensitivity in bladder cancer (41). In this study, we observed that suppression of p53 produced no change in drug sensitivity in one osteosarcoma line and in three renal cancer cell lines while increasing drug susceptibility in another renal carcinoma line. These data again indicate that p53 does not have one defined function in cancer susceptibility to treatment. Cell death or survival depends on the balance among p53-dependent apoptosis, p53-induced senescence, p53-dependent temporary growth arrest, p53-mediated DNA repair as well as the existence of alternative mechanisms preventing mitotic catastrophe (45). This balance is regulated by largely unknown modulators that determine the final outcome of p53 activation in response to drug treatment, many of which are likely to be tissue specific. This indicates that the clinical effect of p53 mutations must be assessed in a tissue context.

Acknowledgments

Received 11/27/2006; revised 8/5/2007; accepted 8/23/2007.

Grant support: NIH grants CA60730 and CA75179 (A.V. Gudkov) and National Health and Medical Research Council and Cancer Institute NSW Grants (M. Haber and M.D. Norris).

The costs of publication of this article were defrayed in part by the payment of page charges. This article must therefore be hereby marked *advertisement* in accordance with 18 U.S.C. Section 1734 solely to indicate this fact.

We thank Dr. Peter Chumakov (Lerner Research Institute, Cleveland Clinic Foundation, Cleveland, OH) for providing valuable reagents and Dr. David Bowtell (Peter MacCallum Cancer Centre, Melbourne, Victoria, Australia) for the microarray analysis.

References

1. Donehower LA, Harvey M, Slagle BL, et al. Mice deficient for p53 are developmentally normal but susceptible to spontaneous tumors. Nature 1992;356:215–21.
2. Oliner JD, Kinzler KW, Meltzer PS, George DL, Vogelstein B. Amplification of a gene encoding a p53-associated protein in human sarcomas. Nature 1992;358:80–3.
3. Momand J, Jung D, Wilczynski S, Niland J. The MDM2 gene amplification database. Nucleic Acids Res 1998;26:3453–9.
4. Scheffner M, Werness BA, Huibregtse JM, Levine AJ, Howley PM. The E6 oncoprotein encoded by human papillomavirus types 16 and 18 promotes the degradation of p53. Cell 1990;63:1129–36.
5. Levine AJ. p53, the cellular gatekeeper for growth and division. Cell 1997;88:323–31.
6. El-Deiry WS. The role of p53 in chemosensitivity and radiosensitivity. Oncogene 2003;22:7486–95.
7. Dimri GP. What has senescence got to do with cancer? Cancer Cell 2005;7:505–12.
8. Erenpreisa J, Kalejs M, Cragg MS. Mitotic catastrophe and endomitosis in tumor cells: an evolutionary key to a molecular solution. Cell Biol Int 2005;29:1012–8.
9. Roninson IB. Tumor cell senescence in cancer treatment. Cancer Res 2003;63:2705–15.
10. Gudkov AV, Komarova EA. The role of p53 in determining sensitivity to radiotherapy. Nat Rev Cancer 2003;3:117–29.
11. Maris JM, Matthay, KK. Molecular biology of neuroblastoma. J Clin Oncol 1999;17:2264–79.
12. Norris MD, Bordow SB, Marshall GM, Haber PS, Cohn SL, Haber M. Expression of the gene for multidrug-resistance-associated protein and outcome in patients with neuroblastoma. N Engl J Med 1996;334:231–8.
13. Haber M, Smith J, Bordow SB, et al. Association of high-level MRP1 expression with poor clinical outcome in a large prospective study of primary neuroblastoma. J Clin Oncol 2006;24:1546–53.
14. Keshelava N, Zuo JJ, Chen P, et al. Loss of p53 function confers high-level multidrug resistance in neuroblastoma cell lines. Cancer Res 2001;61:6185–93.
15. Moll UM, LaQuaglia M, Benard J, Riou G. Wild-type p53 protein undergoes cytoplasmic sequestration in undifferentiated neuroblastomas but not in differentiated tumors. Proc Natl Acad Sci U S A 1995;92:4407–11.
16. Moll UM, Ostermeyer AG, Haladay R, Winkfield B, Frazier M, Zambetti G. Cytoplasmic sequestration of wild-type p53 protein impairs the G1 checkpoint after DNA damage. Mol Cell Biol 1996;16:1126–37.
17. Nikolaev AY, Li M, Puskas N, Qin J, Gu W. Parc: a cytoplasmic anchor for p53. Cell 2003;112:29–40.
18. Haber M, Bordow SB, Gilbert J, et al. Altered expression of the MYCN oncogene modulates MRP gene expression and response to cytotoxic drugs in neuroblastoma cells. Oncogene 1999;18:2777–82.
19. Kondratov RV, Komarov PG, Becker Y, Ewenson A, Gudkov AV. Small molecules that dramatically alter multidrug resistance phenotype by modulating the substrate specificity of P-glycoprotein. Proc Natl Acad Sci U S A 2001;98:14078–83.
20. Bordow SB, Haber M, Madafiglio J, Cheung B, Marshall GM, Norris MD. Expression of the multidrug resistance-associated protein (MRP) gene correlates with amplification and overexpression of the N-myc oncogene in childhood neuroblastoma. Cancer Res 1994;54:5036–40.
21. Kingston RE. Calcium phosphate transfection. In: Ausubel FM, Brent R, Kingston RE, et al. editors. Current protocols in molecular biology. Massachusetts: Wiley Interscience; 1987. p. 9.1.4–6.
22. Boiko AD, Porteous S, Razorenova OV, Krivokrysenko VI, Williams BR, Gudkov AV. A systematic search for downstream mediators of tumor suppressor function of p53 reveals a major role of BTG2 in suppression of Ras-induced transformation. Genes Dev 2006;20:236–2.
23. Grant CE, Valdimarsson G, Hipfner DR, Almquist KC, Cole SPC, Deeley RG. Overexpression of multidrug resistance-associated protein (MRP) increases resistance to natural product drugs. Cancer Res 1994;54:357–61.
24. Murphy KM, Streips UN, Lock RB. Bax membrane insertion during Fas(CD95)-induced apoptosis precedes cytochrome *c* release and is inhibited by Bcl-2. Oncogene 1999;18:5991–9.
25. Dimri G, Lee X, Basile G, et al. A biomarker that identifies senescent human cells in culture and in aging skin *in vivo*. Proc Natl Acad Sci U S A 1995;92:9363–7.
26. Haber M, Norris MD, Kavallaris M, et al. Atypical multidrug resistance in a therapy-induced drug-resistant human leukemia cell line LALW-2 resistance to *Vinca* alkaloids independent of P-glycoprotein. Cancer Res 1989;49:5281–7.
27. Tweddle D, Malcolm A, Bown N, Pearson A, Lunec J. Evidence for the development of p53 mutations after cytotoxic therapy in a neuroblastoma cell line. Cancer Res 2001;61:8–13.
28. Kotchetkov R, Driever PH, Cinatl J, et al. Increased malignant behavior in neuroblastoma cells with acquired multi-drug resistance does not depend on P-gp expression. Int J Oncol 2005;27:1029–37.

29. Layfield LJ, Thompson JK, Dodge RK, Kerns BJ. Prognostic indicators for neuroblastoma: stage, grade, DNA ploidy, MIB-1-proliferation index, p53, HER-2/neu and EGFr-a survival study. J Surg Oncol 1995;59:21–7.
30. Cadwell C, Zambetti GP. The effects of wild-type p53 tumor suppressor activity and mutant p53 gain-of-function on cell growth. Gene 2001;277:15–30.
31. Ossovskaya VS, Mazo IA, Chernov MV, et al. Use of genetic suppressor elements to dissect distinct biological effects of separate p53 domains. Proc Natl Acad Sci U S A 1996;93:10309–14.
32. Mantovani F, Banks L. The human papillomavirus E6 protein and its contribution to malignant progression. Oncogene 2001;20:7874–87.
33. Cimoli G, Malacarne D, Ponassi R, Valenti M, Alberti S, Parodi S. Meta-analysis of the role of p53 status in isogenic systems tested for sensitivity to cytotoxic antineoplastic drugs. Biochim Biophys Acta 2004;1705:103–20.
34. Weinstein JN, Myers TG, Oconnor PM, et al. An information-intensive approach to the molecular pharmacology of cancer. Science 1997;275:343–9.
35. Edelman MJ, Meyers FJ, Miller TR, Williams SG, Gandour-Edwards R, deVere White RW. Phase I/II study of paclitaxel, carboplatin, and methotrexate in advanced transitional cell carcinoma: a well-tolerated regimen with activity independent of p53 mutation. Urology 2000;55:521–5.
36. Giannakakou P, Sackett DL, Ward Y, Webster KR, Blagosklonny MV, Fojo T. p53 is associated with cellular microtubules and is transported to the nucleus by dynein. Nat Cell Biol 2000;2:709–17.
37. Zhang CC, Yang JM, White E, Murphy M, Levine A, Hait WN. The role of MAP4 expression in the sensitivity to paclitaxel and resistance to *Vinca* alkaloids in p53 mutant cells. Oncogene 1998;16:1617–24.
38. McKenzie PP, Guichard SM, Middlemas DS, Ashmun RA, Danks MK, Harris LC. Wild-type p53 can induce p21 and apoptosis in neuroblastoma cells but the DNA damage-induced G_1 checkpoint function is attenuated. Clin Cancer Res 1999;5:4199–207.
39. Tweddle DA, Malcolm AJ, Cole M, Pearson AD, Lunec J. p53 cellular localization and function in neuroblastoma: evidence for defective G(1) arrest despite WAF1 induction in MYCN-amplified cells. Am J Pathol 2001;158:2067–77.
40. Weller M. Predicting response to cancer chemotherapy: the role of p53. Cell Tissue Res 1998;292:435–45.
41. Wallace-Brodeur RR, Lowe SW. Clinical implications of p53 mutations. Cell Mol Life Sci 1999;55:64–75.
42. Peller S, Rotter V. TP53 in hematological cancer: low incidence of mutations with significant clinical relevance. Hum Mutat 2003;21:277–84.
43. Berns EMJJ, Foekens JA, Vossen R, et al. Complete sequencing of TP53 predicts poor response to systemic therapy of advanced breast cancer. Cancer Res 2000;60:2155–62.
44. Reles A, Wen WH, Schmider A, et al. Correlation of p53 mutations with resistance to platinum-based chemotherapy and shortened survival in ovarian cancer. Clin Cancer Res 2001;7:2984–97.
45. Roninson IB, Broude EV, Chang BD. If not apoptosis, then what? Treatment-induced senescence and mitotic catastrophe in tumor cells. Drug Resist Updat 2001;4:303–13.

p53 Determines Multidrug Sensitivity of Childhood Neuroblastoma

Chengyuan Xue, Michelle Haber, Claudia Flemming, et al.

Cancer Res 2007;67:10351-10360.